Ad Hoc Networks 75–76 (2018) 98–105

Contents lists available at ScienceDirect

Ad Hoc Networks

journal homepage: www.elsevier.com/locate/adhoc

On the lifetime analysis of energy harvesting sensor nodes in smart grid environments

H.E. Erdem*, V.C. Gungor

Abdullah Gul University, Computer Engineering Department, Kayseri 38060, Turkey

ARTICLE INFO

Article history:
Available online 22 March 2018

Keywords:
Energy harvesting
Smart grid
Wireless sensor networks

ABSTRACT

Smart grids represent the future of power generation, distribution and transmission systems. Integration of renewable energy sources with fluctuating power output into the grid requires constant monitoring of grid assets. Wireless Sensor Networks (WSNs) provide an efficient monitoring infrastructure for data collection from multiple locations for extended periods. The aim of this study is to investigate the lifetime of the energy harvesting WSN nodes inside a substation, where the sensor nodes exploit the abundant electromagnetic field in the substation environment. Performance results show that the impact of harvesters on node lifetime is crucial compared to available power management systems, when realistic substation channel conditions are considered.

1. Introduction

Traditional grids are replaced with smart grids that enable the incorporation of renewable energy sources without impairing reliability. This integration requires active monitoring of unpredictably fluctuating energy generation and consumption levels to provide efficient distribution of the generated energy and blackout-proof infrastructure. Such monitoring task can be achieved using a scalable network of inexpensive and reliable nodes. In this respect, utilization of Wireless Sensor Networks (WSNs) technology is the most common practice among enabling technologies. Current WSN based smart grid applications include remote monitoring of transmission lines, automatic fault detection, demand and delivery optimization, smart metering, and outage management [1–3].

WSNs consist of multiple nodes with sensor(s), processor(s), and radio hardware integrated in each node. In a smart grid environment, the power supplied to the nodes is usually provided by batteries since powering directly from the grid requires expensive and complicated converter circuits. After a battery is depleted, a replacement procedure has to be initiated. In a smart grid environment, this scenario is not desired due to costs and high electromagnetic/electric field intensities harmful on human body. Moreover, requiring frequent battery replacements may impair data integrity. Therefore, extending node lifetime plays a vital role on diminishing the negative outcomes of monitoring tasks.

Node lifetime can be extended by either increasing the total available energy or decreasing the average power consumption. The former can be accomplished using bigger batteries or energy harvesting devices while the latter is limited to available low power components and power management practices. The scope of this study is limited to energy harvesting devices and power management practices since the utilization of bigger batteries or low power components is limited to application constraints and market availability.

Energy harvesting devices aim to increase total available energy by converting ambient energy into electrical energy and assisting the integrated battery. Ambient energy can be present in various forms, such as electromagnetic, solar, and kinetic with each type requiring a unique harvester design. In a smart grid environment, harvesting from electromagnetic and electric field seems promising due to high current and voltage levels inside the facilities. However, electromagnetic harvesters are found more suitable for smart grid applications considering the physical size and output power it is capable to provide [4]. Consequently, this study focuses solely on electromagnetic harvesters.

Harvesting from electromagnetic waves can be performed using inductive coils or permanent magnets placed inside electromagnetic field. Using coil, the AC voltage induced at the terminals of the coil can be rectified and used to power the sensor node or assist the node battery. Similarly, force is applied on permanent magnets exposed to electromagnetic waves and the force can be used to vibrate a piezoelectric beam and generate voltage at its terminals by attaching the permanent magnet to the tip of a beam.

Moreover, power management methods aim to decrease the average power consumption. This study focuses on two

* Corresponding author.
E-mail addresses: huseyin.erdem@agu.edu.tr (H.E. Erdem), cagri.gungor@agu.edu.tr (V.C. Gungor).

https://doi.org/10.1016/j.adhoc.2018.03.002
1570-8705/

different power management methods namely schedule-driven power management and event-driven power management that introduce sleep cycles and redundant triggering hardware to reach this goal. The methods also enable adapting to different application scenarios by altering their parameters. In summary, the following contributions have been made:

- The impact of two promising energy harvesting devices based on electromagnetic field on sensor node lifetime within a smart grid facility has been analyzed.
- The effects of both schedule-driven and event-driven power management schemes on lifetime of sensor nodes deployed in smart grid environments have been investigated.
- The impact of radio propagation characteristics for different smart grid environments, such as 500 kV outdoor substation Line of Sight (LOS) and Non-Line of Sight (NLOS) environments, on sensor node lifetime have been investigated.

The remainder of this paper is organized as follows. An overview of the available studies for electromagnetic energy harvesting in smart grid environment is presented in Section II. Energy harvesting methods used in this study are introduced in Section III. Section IV provides insight on the power management methods utilized throughout the study. Section V presents the results of the simulations conducted and Section VI concludes the paper.

2. Related work

To date, there have been numerous studies analyzing the feasibility of harvesting device utilization in smart grid environments. In these studies, electromagnetic field harvester is the most common harvester type. However, the mechanisms and the methods used for capturing the ambient electromagnetic energy and converting it into electrical energy vary.

Moghe et al. design a self-sufficient hardware that exploits the magnetic field present in the environment to harvest energy and reports its readings of environmental parameters [5]. The designed harvester requires clamping besides the conductor and enables sensor node to report measured data once in 61 s when 100 A of current flows through the conductor.

Han et al. use a vibrating beam structure with permanent magnet attached to its tip to harvest energy from varying magnetic field of a power line [6]. The alternating torque due to the force AC magnetic field exerts on the magnet is applied on the cantilever beam with piezoelectric material. The electric potential generated along the terminals of the stressed material is used to power the sensor node. The maximum harvested power of 9.40 mW from 40 A of current flow is stated to be more than sufficient to power a low power sensor node.

The authors of [3] adopt the electromagnetic harvester design proposed in [7] to integrate it into sensor node that will energize itself. Their proposed design possesses a cubical structure that will be positioned next to a conductor preventing installation hindrances. Their results show that the harvester is capable to provide 744 mW of power when positioned next to a conductor with 170 A of current.

In [8], the authors propose a multilayered coil structure to harvest electromagnetic energy along with its accurate mathematical model. They show that their design is superior to previous coil designs in terms of harvested energy. They manage to harvest around 10 mW of power from a conductor with 13.5 A current. In addition, the analytical model they suggest provides results within an error margin of 10% compared to practical results.

Another study analyzes the feasibility of utilizing mobile vehicles with electromagnetic wave based wireless charging capabilities to charge the nodes [9]. The routes of the vehicles and the landmark locations to activate charging operations are optimized to meet the energy demand of the nodes with least residual energy while using minimum path traversing.

Roscoe et al. focus on Free-Standing Harvesters (FSHs) where the coil is not necessarily be clamped around a conductor [10]. They state that the magnetic flux levels within substations may be sufficient to energize wireless sensor nodes. According to the results, magnetic flux density level in an ordinary 400 kV indoor substation is sufficient to power a MICAz sensor node performing data transmission every 4 minutes.

Yuan et al. analyze the structure of coil to be used as a harvester when positioned under overhead transmission lines [11]. They propose a novel bow tie shaped coil structure with its proven superiority over traditional cylindrical shape. Optimizing the design further by using the most effective core material among many types, they manage to scavenge 146.7 mW of power when the harvester is positioned 5 m above the ground with a magnetic flux density of 11 μT_{rms}. In addition, an analytical model to calculate the output power is provided.

Another study similar to [6], aims to eliminate the requirement of coil surrounding the conductor by using permanent magnet to convert magnetic energy into mechanical energy [12]. However, the mechanical energy is converted into electrical energy using another permanent magnet-coil pairs instead of a piezoelectric cantilever used in [6]. This way, they manage to harvest 0.16 mW of power from a conductor with 50 A of current. Although the output power is reduced greatly, they suggest that not using piezoelectric material on a continuously vibrating beam increases the durability of the system.

Table 1 shows a summary of energy harvesting methods based on electromagnetic field. Although these studies provide valuable insights on the contribution harvesters make, they do not evaluate how the contribution is affected under different usage scenarios. In our previous work, the harvesters are tested in NLOS smart grid environment using event driven scheme [13]. In this study, we carry the experiment further by incorporating schedule driven scheme and LOS smart grid environments. This way, lifetime analysis with different duty cycle ratios and event arrival rates is enabled.

3. Energy harvesting methods

Energy harvesting aims to generate electrical energy using various types of hardware exploiting ubiquitous energy resources present in the environment. This study focuses on electromagnetic field harvesters utilized to assist integrated batteries of a sensor node inside smart grid environment. In this study, electromagnetic harvesters called Conductor Winding Harvester (CWH) and Free Standing Harvester (FSH) are used.

The first harvester type is clamped around a current carrying conductor exploiting the energy of electromagnetic field generated due to current flow. The device harvests the electromagnetic energy using an inductive coil with its cross sectional area overlapping the electromagnetic field's circular area. Such design is especially useful for monitoring conductor voltage, current or temperature levels.

The second harvester type focuses on cases where clamping around a conductor is not feasible or the locations at which the parameters are measured do not contain conductors within their close proximity. Being positioned away from a conductor, the assumption of overlapping the coil cross sectional area and electromagnetic field's circular area loses its validity. Although this usually causes lower output power, having a wider physical space available allows using bigger coils.

Table 1
Electromagnetic harvesting methods in smart grids.

Harvester position	Energy resource	Harvester hardware
Near conductor (non-intrusive) [5]	Current carrying conductor	Coil
Near conductor (non-intrusive) [6]	Current carrying conductor	Piezoelectric cantilever with permanent magnet
Near conductor (non-intrusive) [7]	Current carrying conductor	Coil
Clamped around the conductor (intrusive) [8]	Current carrying conductor	Coil
Inside substation [9]	Mobile charging vehicle	–
Near conductor (non-intrusive) [10]	Current carrying conductor	Coil
Near conductor (non-intrusive) [11]	Current carrying conductor	Coil
Near conductor (non-intrusive) [12]	Current carrying conductor	Permanent magnet-coil pair

In this study, analyses are conducted considering harvesters placed inside a substation or clamped around a conductor. Following sections provide detailed information on harvesters.

3.1. Conductor winding harvester

This type of harvester consists of a coil surrounding the conductor to harvest electrical energy. The current generated electromagnetic field induces AC voltage at the terminals of the coil. The magnitude of this voltage is directly proportional to the change in the magnetic flux. This relation is shown in (1).

$$V = \frac{d\Phi}{dt} \tag{1}$$

In (1), Φ represents the total magnetic flux on the entire coil.

In [8] multilayered core structure is proven superior to single layered structure. Therefore, the core structure presented in the mentioned study is used as the reference model. According to this model, the RMS voltage induced at the terminals can be estimated using:

$$V_{coil} = N\mu_0\mu_r\omega f I \ln\left(1 + \frac{h}{r}\right) \tag{2}$$

where N and r represent the number of turns and the distance of the coil from the conductor. Moreover, μ_r, ω and h represent the relative permeability, width and the thickness of the core material, respectively. In addition, I and f represent the RMS magnitude and the current frequency.

The relative permeability parameter (μ_r) in (2) does not consider the air gap of the core material. To incorporate the gap consideration, below formula is used [8]:

$$\mu_{rg} = \frac{C}{\frac{1}{\frac{A}{l_g} + \left(0.241 + \frac{1}{\pi}\ln\frac{b}{l_g}\right)P} + \frac{C}{\mu_r}} \tag{3}$$

where C parameter represents:

$$C = l_m/A \tag{4}$$

In (3) and (4), parameters A, P, b, l_g and l_m represent core cross-sectional area, core cross-sectional perimeter, half the inner core perimeter, gap length, and average core perimeter without the gap, respectively. The l_m parameter can be calculated more precisely using:

$$l_m = l_a - l_g = \frac{\pi(D_o - D_i)}{ln\left(\frac{D_o}{D_i}\right)} - l_g \tag{5}$$

where l_a, D_o and D_i represent average core perimeter, outer and inner core diameter, respectively.

In addition to gap consideration, multilayered core structure also affects the core permeability. Therefore, (6) improves (3) even further considering an n-layered core structure:

$$\mu_{rgn} = 1 + (\mu_{rg} - 1)\frac{nd}{T} \tag{6}$$

In (6), parameters n, d and T represent the number of core layers, thickness of a single core layer and thickness of the entire core, respectively. The μ_r parameter in (2) is replaced with the calculated μ_{rgn} parameter for improved accuracy.

Maximum power delivery requires the load resistance to be equal to the coil resistance. The power delivered to the load using half the AC voltage induced on the load resistance can be calculated using (7) [11]:

$$P = \frac{\left(\frac{V_{coil}}{2}\right)^2}{R_{coil}} \tag{7}$$

In (7), R_{coil} can be assumed as only copper resistance [11]. The copper resistance can be calculated as in (8) [11].

$$R_{copper} = 2\pi(0.5D_o)N\rho + \frac{\pi N^2 {d_{wire}}^2 \rho}{L} \tag{8}$$

In (8), ρ, d_{wire} and L represent resistivity and diameter of the winding wire and the length of the core.

3.2. Free standing harvester

In cases where using CWH is not feasible or the locations of the necessary measurements require positioning away from conductors, FSHs can be utilized. This harvester type scavenges the available electromagnetic field without being clamped around a conductor. Hence, the coil cross-sectional area and the circular area of the magnetic field created by the current do not overlap, unlike the previous case. Therefore, the small core gap assumption made for the conductor clamped harvester in (3) is invalid. The revocation of overlapping magnetic field and coil cross section renders a new mathematical model mandatory. According to the new model proposed in [10], the maximum output voltage of a coil inside a non-overlapping magnetic flux is given as:

$$V_{coil} = 2\pi f \mu_{eff} N\pi (0.5D)^2 B \tag{9}$$

Where B represent magnetic flux density. The output power can be calculated using (7). Combining (9) and (7), the output power of the coil can be calculated using:

$$P = \frac{\left(\pi^2 N(0.5D)^2\right)^2}{R_{coil}} {\mu_{eff}}^2 (fB)^2 \tag{10}$$

In addition to various energy harvesters, this study also considers different power management schemes and a realistic channel model for the smart grid environment. These aspects of the study are presented in the following sections.

4. Power management schemes

Harvesters are capable to increase the amount of total available energy. However, efficient usage of the available energy is also vital for extended lifetime. Power management schemes play a significant role in providing lower power consumption levels. In

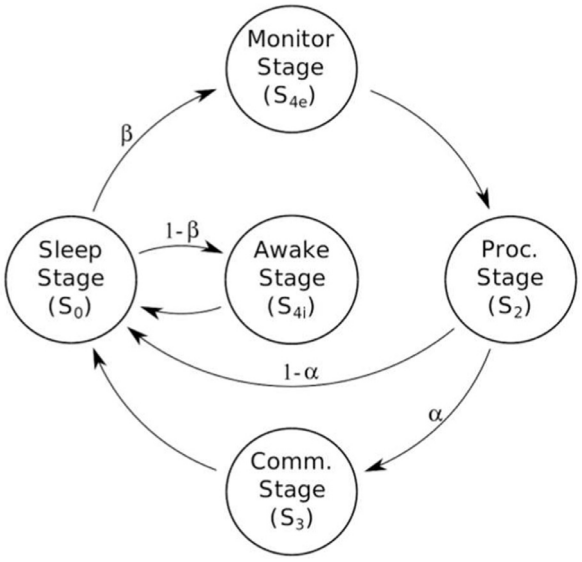

Fig. 1. Operational workflow of schedule driven scheme.

Table 2
Hardware statuses for schedule driven scheme states.

State	Radio	CPU	Sensor
S_0	OFF	OFF	OFF
S_1	–	–	–
S_2	OFF	ON	ON
S_3	TX	ON	OFF
S_4	OFF	IDLE	ON
S_5	RX	ON	OFF

this study, lifetime of Telos sensor mote with different harvesting modules is analyzed using schedule driven and event driven power management methods using MATSNL toolbox [14]. The toolbox helps analyze node lifetime using consecutively executed tasks represented as individual states. The following subsections provide detailed information on these power management schemes.

4.1. Schedule driven scheme

One of the most common methods for decreased power consumption is using sleep intervals. Schedule driven power management scheme improves this rule by incorporating individual activation of hardware components according to node states representing different tasks.

In this scheme, entire lifecycle of a mote is considered to possess four distinct tasks: sleeping, sensing, computation and communication. The transitions among these tasks while the node is awake are shown in Fig. 1. In the figure, successful transmission and event detection probabilities are represented with α and β coefficients, respectively.

The four tasks shown in the figure and sleeping task are represented using five Markov states. The states and the statuses of the hardware components for each state are shown in Table 2. In the table, S_0 represents sleeping, S_2 and S_4 represent processing and sensing, S_3 and S_5 represent transmission and reception states. The time to enter and exit S_0 (sleeping state) is determined using Real Time Clock (RTC) Integrated Circuit (IC) and predefined intervals based on application specific duty cycle value.

A simple method for lifetime calculation requires dividing the total available energy with the average power consumption:

$$Lifetime = \frac{E_{total}}{P_{avg}} \tag{11}$$

Table 3
Hardware statuses for event driven scheme states.

State	Radio	CPU	Preprocessor	Sensor
S_0	–	–	–	–
S_1	OFF	OFF	ON	OFF
S_2	OFF	ON	ON	ON
S_3	TX	ON	ON	OFF
S_4	OFF	IDLE	ON	ON
S_5	RX	ON	ON	OFF

The average power consumption for a sensor node should be determined considering state entrance possibilities and hardware statuses inside these states since each state has a different power consumption value due to variations in active hardware components. Moreover, the duration of each state affects state power consumptions further. Eq. (12) shows the average power consumption formula.

$$P_{avg} = \frac{P_e + \frac{\beta}{T_c} E_e}{1 + \frac{\beta}{T_c} T_e} \tag{12}$$

In (12), P_e represents the power consumption when no event is detected. E_e and T_e represent additional energy and time spent in case of event detection. Finally, β and T_c represent event detection probability and cycle duration. The average power consumption without event detection is calculated via:

$$P_e = P_{S_0} + d\left(P_{S_4} - P_{S_0}\right) + \frac{C_P}{T_C} \tag{13}$$

where P_{S_i}, C_P and T_C represent the power spent in the i^{th} state, CPU wake-up cost and cycle duration, respectively. Moreover, average additional time, T_e, in (12) is calculated using:

$$T_e = \overline{N_\sigma}\left(\bar{\sigma} + \bar{Y}\right) + \alpha\overline{N_P}\left(\bar{L} + \bar{Z}\right) - \frac{dT_C(dT_C + 2T_{ev})}{2(dT_C + T_{ev})} \tag{14}$$

where $\overline{N_\sigma}$ is the mean idle state amount, $\bar{\sigma}$ is the average idle state duration, $\bar{Y}$ is the mean processing time per packet, $\overline{N_P}$ is the mean processing state amount, $\bar{L}$ is the mean channel listening duration, $\bar{Z}$ is the mean transmission time per packet and T_{ev} is the event duration.

The additional energy spent, E_e, is calculated via:

$$E_e = \overline{N_\sigma}\left(\bar{\sigma}P_{S_4} + \bar{Y}P_{S_2}\right) + \alpha\overline{N_L}\left(\bar{L}P_{S_5} + \bar{Z}P_{S_3}\right) + C_R - \frac{dT_C(dT_C + 2T_{ev})}{2(dT_C + T_{ev})}P_{S_4} \tag{15}$$

where C_R stands for radio wake-up energy cost.

4.2. Event driven scheme

Although schedule driven scheme is capable to provide improved lifetime results, adoption of sleep cycles is not preferred in applications intolerant to event miss. Therefore, event driven scheme introduces redundant low power hardware responsible for event detection and wakening of the sensor node. Always on redundant hardware enables sensor node stay asleep as long as no event is present. This way, the power consumption is reduced while missing event detection is not risked, whereas, hardware costs are increased.

Similar to previous scheme, event driven scheme also has 5 distinct states for idling, monitoring, computing and communicating tasks. The hardware statuses for these states are listed in Table 3. In addition, state transition diagram is shown in Fig. 2.

Average power consumption is calculated using (16).

$$P_{avg} = \frac{P_{S_1} + \lambda E_e}{1 + \lambda T_e} \tag{16}$$

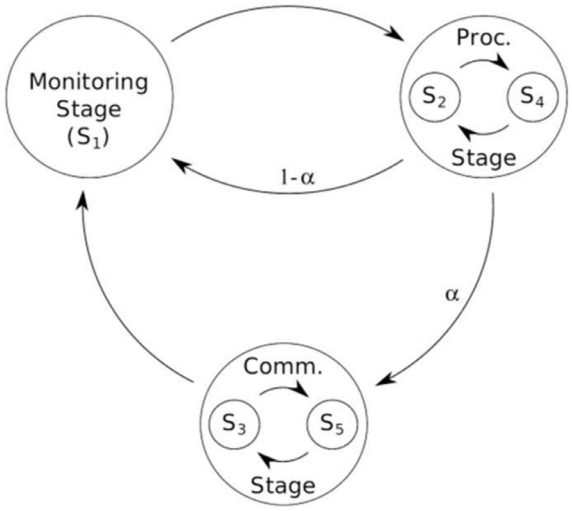

Fig. 2. Operational workflow of event driven scheme.

In (16), P_{S_1} and λ represent the energy spent while idling with active redundant hardware and event arrival rate, respectively. Additional energy and time spent in case of event detection can be calculated via:

$$E_e = \overline{N_\sigma}\left(\bar{\sigma} P_{S_4} + \bar{Y} P_{S_2}\right) + \alpha \overline{N_L}\left(\bar{L} P_{S_5} + \bar{Z} P_{S_3}\right) + C_P + \alpha C_R \tag{17}$$

$$T_e = \overline{N_\sigma}\left(\bar{\sigma} + \bar{Y}\right) + \alpha \overline{N_L}\left(\bar{L} + \bar{Z}\right) \tag{18}$$

where, N_σ, Y, N_L, L, Z, C_P represent average number of jobs per event, average processing time per event, average channel listening time, average transmission time per packet, and CPU wake-up energy cost, respectively.

5. Channel model

Last but not the least, environmental conditions that affect the communication channel behavior should be taken into account. Channel conditions may cause different attenuation and fading behaviors that affects successful reception of a package. In case of a transmission failure, retransmission of the package is common. However, the impact of retransmissions on lifetime is quite high since the power consumption of transmission task is a lot higher than that of processing and sensing tasks. Therefore, the number of retransmissions has to be taken into consideration.

In this study, log normal shadowing is the preferred method for modeling the communication channel and predict the number of retransmissions. Using the model, firstly the path loss at the desired distance is calculated based on the path loss measurements at a reference distance.

$$PL(d)[dB] = \overline{PL}(d_0) + 10\eta log\left(\frac{d}{d_0}\right) + X_\sigma \tag{19}$$

In (19), $\overline{PL}(d_0)$ represent the path loss at a reference distance. In addition, d, n, and X_σ represent distance, path loss exponent and Gaussian random variable with shadowing standard deviation σ and zero mean.

Moreover, not all the smart grid environments have the same behavior. Therefore, this study focuses on LOS and NLOS environments. While LOS environments enable unobstructed communication between the transmitter and the receiver, NLOS environments are able to allow communication only through reflections.

In this study, path loss at reference distance is adopted from [15] while path loss exponent and shadowing deviation parameters for LOS and NLOS environments are adopted from [16], which measures the parameters in field trials conducted at a 500 kV substation in Georgia Power facilities in Atlanta, USA. The parameters are listed in Table 6.

Table 4
Simulation parameters for CWH.

Parameter	Value	Unit
Coil turns (N)	280	–
Current (I)	13.5	A
Gap length (l_g)	1	mm
Relative permeability (μ_r)	1×10^5	H/m
Resistivity (ρ)	1.11	Ω/m

Table 5
Simulation parameters for FSH.

Parameter	Value	Unit
Magnetic flux density (B)	10	μT (rms)
Coil turns (N)	10,000	–
Effective permeability (μ_{eff})	23	H/m

After the path loss calculation, Signal to Noise Ratio (SNR) parameter is calculated using:

$$\gamma(d)_{dB} = P_t - PL(d) - P_n \tag{20}$$

In (20), γ, P_t and P_n represent SNR, transmission power and noise floor parameters. The output power is 0 dBm while the noise floor is −93 dBm [18]. The calculated SNR value is then used to calculate Bit Error Rate (BER) value:

$$P_b = Q(E_b/N_{0DS}) \tag{21}$$

In (21), E_b/N_{0DS} represent SNR per bit value and found using [15]:

$$\frac{E_b}{N_0} = SNR\frac{B_N}{R} \tag{22}$$

In (22), B_N and R parameters represent noise bandwidth and data rate values. The BER can finally be used to calculate PRR value, which allows calculation of retransmissions.

$$PRR = (1 - P_b)^{8l}(1 - P_b)^{8(f-l)} \tag{23}$$

In (23), f and l parameters represent frame size and preamble. Retransmissions are limited to three to prevent high retransmission numbers that degrade lifetime extremely under poor conditions.

6. Results

Using the technical approaches mentioned in the previous sections, lifetime of a sensor node have been evaluated based on two different harvesting devices and power management schemes on Telos mote. According to the scenario assumed, there happens multiple events with predefined intervals and the sensor node tries to detect the event and send its measurements to a sink node located at a predefined distance.

The harvesters are assumed to be located inside a 500 kV substation. The CWH is assumed to be clamped around a conductor, while the FSH is positioned inside the substation.

Simulation parameters for CWH and FSH are listed in Tables 4 and 5. One of the most important parameters for FSH output power calculation is the magnetic flux density levels. Within a substation, this value may show variations among locations. Therefore, in this study approximate mean value of field measurements obtained by walking inside substation [17] is adopted. The study conducted by Tanaka et al. provides magnetic flux density levels measured at 1 m height continuously while walking inside a substation.

The parameters used for propagation model are listed in Table 6. Path loss exponent, shadowing standard deviation and

Table 6
Simulation parameters for log-normal shadowing model.

Parameter	Value	Unit
Reference path loss ($\overline{PL}$ (d_0))	55	dB
Reference distance (d_0)	1	m
Frame length (f)	30	Bytes
Preamble length (l)	2	Bytes
Path loss exponent (η) *(LOS)*	2.42	–
Path loss exponent (η) *(NLOS)*	3.51	–
Shadowing standard deviation (σ) *(LOS)*	3.12	–
Shadowing standard deviation (σ) *(NLOS)*	2.95	–
Noise floor (P_n)	−93	dB
Radio output power (P_t)	0	dBm

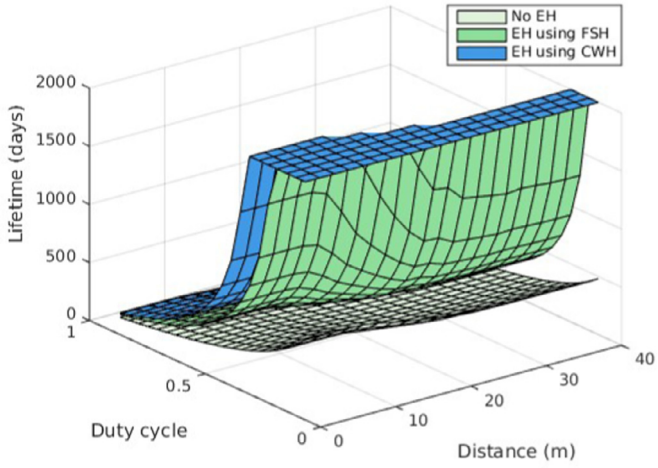

Fig. 3. Lifetime using FSH and CWH with schedule driven scheme in LOS environment.

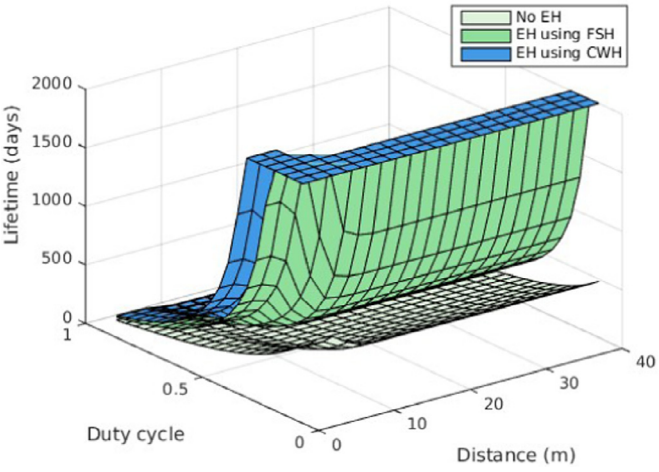

Fig. 4. Lifetime using FSH and CWH with schedule driven scheme in NLOS environment.

noise floor parameters for LOS NLOS environments in the table are adopted from [15] which provides field measurements in smart grid environments. In a LOS environment, the receiver and transmitter nodes are placed within direct sight of each other while in an NLOS environment there are physical obstructions between them.

The graphs from Figs. 3 to 6 demonstrate the results with lifetime values capped at 2000 days using different power management schemes and channel parameters. While the event driven scheme uses varying event arrival rates, the schedule driven scheme uses 600 event arrivals per day.

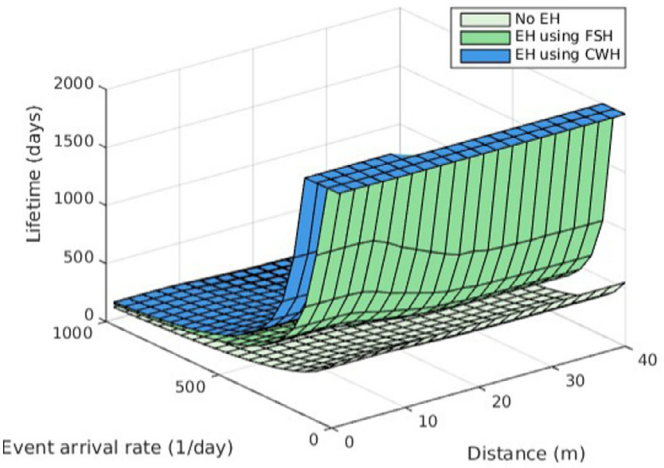

Fig. 5. Lifetime using FSH and CWH with event driven scheme in LOS environment.

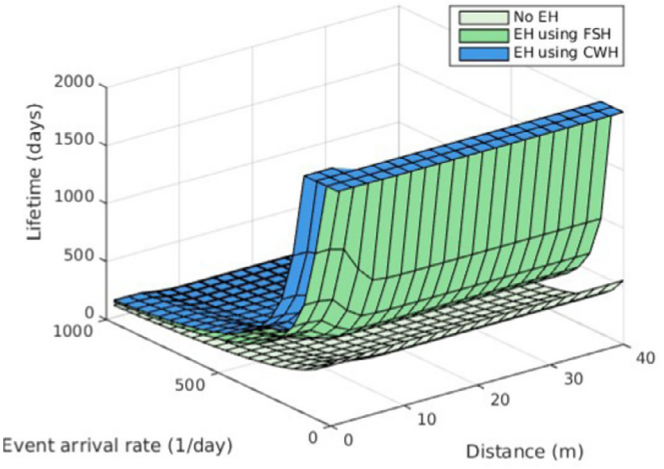

Fig. 6. Lifetime using FSH and CWH with event driven scheme in NLOS environment.

In all performance results, CWH outperforms FSH with the highest contribution at low duty cycle or event arrival rates. In these regions, the overall average power consumption of the node is decreased, rendering the magnitude of the harvested power relatively greater. Therefore, using the same amount of harvested power, the lifetime is not improved much in other regions.

Although CWH provides slightly higher power output, the power to volume ratio of the CWH is much higher than that of FSH due to huge size of the FSH compared to CWH. This is the result of stricter size constraints on CWH to prevent the sagging of the conductor. Moreover, the location of the FSH within substation is another factor to be considered. Based on the application type, the positioning of the FSH may vary depending on the parameter to be measured. Although this study uses median magnetic flux density value, the magnitude of the harvested power may be lower/higher based on the harvester location. In addition, magnetic flux levels may vary throughout the day causing fluctuations in harvester power output.

Comparing the impacts of different power management schemes, the duty cycle value plays a vital role. Duty cycle value for schedule driven scheme represents the ratio of node being awake to being asleep. Therefore, a node using schedule driven scheme will miss the events happening while it is asleep as opposed to event driven scheme. For this reason, to compare the power management schemes, lifetime values at maximum duty cycle values should be used. Moreover, the schedule driven scheme

is tested using 600 daily event arrivals. As a result, using duty cycle of 1 and daily events of 600, the lifetime schedule and event driven schemes provide at 5 m of transmission distance are 140 and 259 days, respectively. Therefore, the contribution redundant low power hardware provides is exceptional. However, if the application is tolerant to missed events, using schedule driven scheme with lower duty cycle values provide better results overall.

Along the distance axis, there is a special region in which lifetime decreases. The distances this trend starts and ends represent the limits at which minimum number of retransmissions ends and maximum number of retransmission starts, respectively. In Fig. 3, up to around 7 m of distance, single transmission occurs. Between the distances of 7 m and 25 m, the number of transmissions is increased up to the maximum limit of 3. Beyond 25 m, successful transmission is not guaranteed, since a successful transmission requires more than the maximum number of retransmissions permitted. In NLOS environments, the distances for lower and upper limits of the transitional region are shorter. This is mainly due to harsher channel conditions represented with higher path loss exponent. As a result, LOS environments tend to provide longer lifetime at higher distances.

To sum up, energy harvesters enable much longer lifetime for sensor nodes using both power management schemes. Although CWH performs better, it is an intrusive method and may not be applicable to all applications. In addition, the NLOS environment goes into the transitional region in shorter ranges, rendering it with shorter lifetime due to having higher retransmission numbers. However, after reaching the maximum allowed retransmission number, both environments settle at the same lifetime durations in a disconnected region.

7. Conclusions and future work

Powering the monitoring nodes in smart grids is a crucial topic to encourage further development. This paper presents that energy harvesting is a viable solution to lifetime problem of sensor nodes when used with proper power management methods. Various environments with different propagation characteristics may affect PRR and retransmission numbers. Thus, the location and width of the transitional region may show differences among environments. Performance results show that NLOS environment with higher path loss exponent usually provide shorter lifetime for sensor nodes.

Performance results also show that CWH can improve lifetime by using low duty cycle values or inter arrival rates. It should be noted that simulations in this study consider only 10A of current flow through the conductor. In case of higher flows, CWH can extend the duty cycle range where infinite lifetime is guaranteed.

This study focuses solely on substation environments as a smart grid asset. However, other assets and transmission lines outside the substation also require monitoring to expand reliability beyond substations. However, these structures cover great distances and require multi-hop communication, which is out of the scope of this study. Therefore, the study can be carried further considering harvesting possibilities outside the substation with multi-hop data forwarding.

Acknowledgment

The work of V.C. Gungor was supported by AGUV and BAGEP.

References

[1] B. Fateh, M. Govindarasu, V. Ajjarapu, Wireless network design for transmission line monitoring in smart grid, IEEE Trans. Smart Grid 4 (2) (2013) 1076–1086.
[2] M. Erol-Kantarci, H.T. Mouftah, Wireless Sensor networks for cost-efficient residential energy management in the smart grid, IEEE Trans. Smart Grid 2 (2) (2011) 314–325.
[3] F. Cai, E. Farantatos, R. Huang, A.S. Meliopoulos, J. Papapolymerou, Self-powered smart meter with synchronized data, in: Proceedings of the 2012 IEEE Radio and Wireless Symposium, Santa Clara, CA, 2012.
[4] R. Moghe, Y. Yang, F. Lambert, D. Divan, A scoping study of electric and magnetic field energy harvesting for wireless sensor networks in power system applications, in: Proceedings of the Energy Conversion Congress and Exposition, San Jose, CA, 2009 2009.
[5] R. Moghe, F.C. Lambert, D. Divan, Smart "Stick-on" sensors for the smart grid, IEEE Trans. Smart Grid 3 (1) (2012) 241–252.
[6] J. Han, J. Hu, Y. Yang, Z. Wang, S.X. Wang, J. He, A nonintrusive power supply design for self-powered sensor networks in the smart grid by scavenging energy from AC power line, IEEE Trans. Ind. Electron. 62 (7) (2015) 4398–4407.
[7] F. Cai, D.J. Chung, E. Farantatos, A.S. Meliopoulos, J. Papapolymerou, Self-powered advanced meter design, in: Proceedings of the 2010 Asia-Pacific Microwave Conference, Yokohama, 2010.
[8] R.H. Bhuiyan, R.A. Dougal, M. Ali, A miniature energy harvesting device for wireless sensors in electric power system, IEEE Sensors J. 10 (7) (2010) 1249–1258.
[9] M. Erol-Kantarci, H.T. Mouftah, Suresense: sustainable wireless rechargeable sensor networks for the smart grid, IEEE Wirel. Commun. 19 (3) (2012) 30–36.
[10] N.M. Roscoe, M.D. Judd, Harvesting energy From magnetic fields to power condition monitoring sensors, IEEE Sensors J. 13 (6) (2013) 2263–2270.
[11] S. Yuan, Y. Huang, J. Zhou, Q. Xu, C. Song, P. Thompson, Magnetic field energy harvesting under overhead power lines, IEEE Trans. Power Electron. 30 (11) (2015) 6191–6202.
[12] T. Hosseinimehr, A. Tabesh, Magnetic field energy harvesting from AC lines for powering wireless sensor nodes in smart grids, IEEE Trans. Ind. Electron. 63 (8) (2016) 4947–4954.
[13] H.E. Erdem, V.C. Gungor, Analyzing lifetime of energy harvesting sensor nodes in smart grid environment, in: Proceedings of the First Inernational Balkan Conference on Communications and Networking. 2017, Tirana, 2017.
[14] D. Jung, T. Teixeira, A. Savvides, Sensor node lifetime analysis: models and tools, ACM Trans. Sensor Netw. 5 (1) (2009) 1–33.
[15] M. Zuniga, B. Krishnamachari, Analyzing the transitional region in low power wireless links, in: Proceedings of the 2004 First Annual IEEE Communications Society Conference on Sensor and Ad Hoc Communications Netw., 2004, IEEE SECON, 2004 *2004*.
[16] V.C. Gungor, B. Lu, G.P. Hancke, Opportunities and challenges of wireless sensor networks in smart grid, IEEE Trans. Ind. Electron. 57 (10) (2010) 3557–3564.
[17] K. Tanaka, M. Yukio, N. Katsuhiko, Measurement of power frequency electric and magnetic fields near power facilities in several countries, IEEE Trans. Power Deliv. 26 (3) (2011) 1508–1513.
[18] R. Moghe, A. Iyer, F.C. Lambert, D. Divan, A low-cost electric field energy harvester for an MV/HV asset-monitoring smart sensor, IEEE Trans. Ind. Appl. 51 (2) (2015) 1828–1836.

H. Emre Erdem received his M.Sc. degree in Autonomous Robotics Engineering from University of York, UK in 2014 and is currently a Ph.D. student in Electrical and Computer Engineering program at Abdullah Gul University, Turkey. His current research areas include Wireless Sensor Networks and Underwater Acoustic Networks.

V. Cagri Gungor received his B.S. and M.S. degrees in Electrical and Electronics Engineering from Middle East Technical University, Ankara, Turkey, in 2001 and 2003, respectively. He received his Ph.D. degree in electrical and computer engineering from the Broadband and Wireless Networking Laboratory, Georgia Institute of Technology, Atlanta, GA, USA, in 2007. Currently, he is an Associate Professor and Chair of Computer Engineering Department, Abdullah Gul University (AGU), Kayseri, Turkey. His current research interests are in next-generation wireless networks, wireless ad hoc and sensor networks, smart grid communications, and underwater networks.